Proceedings of the 10th International Conference on Civil Structural and Transportation Engineering (ICCSTE 2025)
July, 2025 | Imperial College London Conference Center, London, United Kingdom
Paper No. 197
DOI:10.11159/iccste25.197

Sustainability, Economy, Efficiency: Parametric Design of Prestressed Slabs for Housing

Bolívar Hernán Maza[1], Daniela Maza Vivanco[2]
[1]Universidad Técnica Particular de Loja
Loja, Loja, Ecuador
bhmaza@utpl.edu.ec
[2]Universidad Técnica Particular de Loja
Loja, Loja, Ecuador
dsmaza@utpl.edu.ec

Abstract **-** Relevant studies reveal that the resistant section of the improperly designed prestressed concrete floor slab reduces adhesion, results in the loss of tensile stress in the steel and concrete, and diminishes shear capacity. Consequently, the service life of the structure decreases. The objective of this work is to analyze the parametric system of the prestressed concrete floor slab for residential floors. The methodology employs static equations to define an efficiency coefficient ξ, which accounts for the static and symmetrical competitiveness of the element, evaluates the position of the centroid (v'_{pl}), and the centroidal inertial (I_{pl}), Variables that assess the number of depressions or semicircles (n_{sc}), width (b), their radii (h_2), thickness of the slab under the depressions (h_1), slab area (A_{pl}). and others are considered. It was found that the factor ξ for the combination $n_{sc} = 6$ y $h_1 = 40\ mm$ is clearly superior, with a confidence interval of 10.75 a 11.05. The greater thickness $h_1 = 40\ mm$ provides higher values of ξ, indicating an increase in rigidity and structural capacity. It is reported that in projects where structural efficiency is prioritized, the configuration $n_{sc} = 6$ *con* $h_1 = 40\ mm$

Keywords**: Prestressed slab; Structural efficiency; Sustainability; Geometric optimization**

1. Introduction

During the study of the service stage of the slab under the effect of characteristic loads, which is perhaps the most restrictive loading stage, the influence of the geometric characteristics of the resistant section is of paramount importance. Above all, it ensures the operational lifespan of the residence by applying innovation and technologies to meet the quality of accommodation and human needs [1]. In this context, the position of the centroid (v'_{pl}) and the centroidal inertia (I_{pl}), especially the latter, define the number of depressions or semicircles (n_{sc}),, width (b)their radii (h_2)thickness of the slab under the depressions (h_1) and the slab area (A_{pl}). Instantaneous vertical deflections account for geometric changes in the resistant structure or prestressed slab, motivated by stress losses, cable relaxation, creep, shrinkage, temperature, and [2]. Efforts are made to define the number of depressions (n_{sc}) that should be made in the slab. In this case, the dimensions of the resistant section reduce its weight (concrete mass) while ensuring that its geometric properties are not significantly weakened. Prefabricated construction induces economic and environmental reductions, high constructive efficiency, and excellent quality of prefabricated elements [2]. It is useful to define an efficiency coefficient in fulfilling the service life and recognizing the symmetrical competitiveness of the element when 6 semicircles $(n_{sc} = 6)$ or 7 semicircles $(n_{sc} = 7)$ are implemented, where symmetry plays a crucial role. [3] ensures that increasing the prestressing force asymmetrically on the resistant section of the prestressed concrete slab increases the vibration frequency.

2. Materials and Methods

If the width of the prestressed concrete slab is defined as $b = 495mm$ in all variants, the dimensionless coefficient ξ that evaluates the section's efficiency will be defined based on the following ratio::

$$\xi = \frac{I_{pl}}{A_{pl} \cdot b^2} \qquad (1)$$

It is observed that ξ assesses the magnitude of the centroidal inertia $\left(I_{pl}\right)$ of the resistant section relative to the cross-sectional area of the concrete element. The inverse factor $\left(b^2\right)$ ensures the dimension lessness of ξ

The geometric properties of the slab's cross-section that are evaluated include:

- ✓ Net section area $\left(A_{pl}\right)$
- ✓ Centroid position $\left(v_{pl},\ v'_{pl}\right)$
- ✓ Centroidal moment of inertia $\left(I_{pl}\right)$
- ✓ Section moduli corresponding to the extreme fibers of the section $\left(W_{pl},\ W'_{pl}\right)$

The characteristics evaluated for a rectangular section are well-known. The proposed criterion is to circumscribe the slab within a rectangular section of equal width and height to that of the slab and to evaluate these magnitudes precisely in the virtual rectangular section. Subsequently, the values corresponding to each of the semicircles (6 or 7, including the two quarter-circles it possesses) are subtracted from them. Since the semicircle is a less frequently addressed figure in the literature, its attributes are defined here. La figura 1, ilustra uno de los semicírculos que aparecen en cada prelosa, todos del mismo radio $r = h_2 = \emptyset/2$.

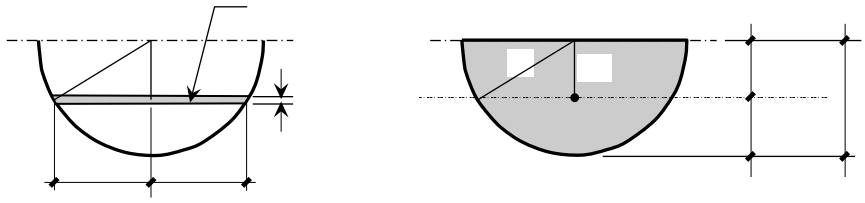

Fig. 1. Location of the centroid in one of the semicircles of the slab.

The area of each semicircle is governed by equation (2), while the position of the centroid of each semicircle is strategic with respect to the horizontal diameter, as shown in Figure 1

$$A_{sc} = \pi\left(h_2\right)^2/2 = 0.5\,\pi h_2^2 \qquad (2)$$

$\bar{y}_{sc} = S_x/A$ (Position of the centroid of the semicircle with respect to its horizontal diameter)
$S_x = \int_0^r y\,dA$ (Static moment of the semicircle with respect to its horizontal diameter)

$dA = (2x)\,dy = \left(2\sqrt{r^2 - y^2}\right)dy$ (diferencial de área)

$$\therefore\ S_x = \int_0^r 2y\left(\sqrt{r^2 - y^2}\right)dy = 2\left(-\frac{1}{3}\sqrt{(r^2 - y^2)^3}\right)\Bigg|_0^r = 2\left(\frac{1}{3}\sqrt{(r^2 - y^2)^3}\right)\Bigg|_r^0$$

$S_x = 2r^3/3$

$$\bar{y}_{sc} = \frac{2r^3/3}{\pi r^2/2} = 0.42r = 0.42h_2 \qquad (3)$$

The following analysis covers the position of the centroidal inertia of the semicircle. $I_{\bar{x}} = \int_{-0.58r}^{0.42r} y^2\, dA$

$$I_{\bar{x}} = \int_{-0.58r}^{0.42r} 2y^2\left(\sqrt{r^2 - y^2}\right) dy = 2\left(-\frac{y}{4}\sqrt{(r^2 - y^2)^3}\right) + \frac{r^2}{8}\left(y\sqrt{(r^2 - y^2)} + r^2 \operatorname{arcsen}\frac{y}{r}\right)\Bigg|_0^r$$

$$I_{\bar{x}} = 0.202 r^4 = 0.202\left(h_2\right)^4 \qquad (4)$$

Having defined the geometric entities of the semicircles that represent the depressions made in the slab during its execution (area, centroid position, and centroidal inertia), all as functions of their radius $\left(r = h_2\right)$, the conditions are established to deduce the same mechanical entities of the slab as a whole. Resources are presented for the deduction of geometric properties of the resistant section.

Net Area.

$$A_{pl} = bh_{pl} - 0.5\, n_{sc} \pi h_2^2 \qquad (5)$$

Where:

$$h_{pl} = h_1 + h_2 \qquad (6)$$

The position of the centroid of the slab is presented in Figure 2, conceived with respect to the lower fiber of the slab represented by the variable v'_{pl}

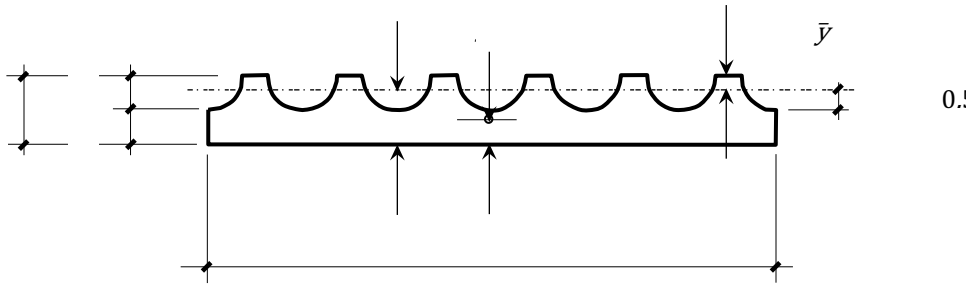

Fig.2. Position of the centroid of the slab with respect to the lower fiber of the slab.

$$v'_{pl} = \frac{\sum S_i}{\sum A_i} = \frac{\sum A_i \cdot \bar{y}_i}{\sum A_i} = \frac{A_{\substack{(prelosa \\ maciza)}} \cdot \bar{y}_{\substack{(prelosa \\ maciza)}} - n_{sc}\left[A_{(sc)} \cdot \bar{y}_{1\,(sc)}\right]}{A_{\substack{(prelosa \\ maciza)}} - n_{sc}\left[A_{(sc)}\right]}$$

$$v'_{pl} = \frac{\left(bh_{pl}\right)\left(h_{pl}/2\right) - n_{sc}\left(\pi h_2^2/2\right)\left(\bar{y}_{(sc)}\right)}{bh_{pl} - n_{sc}\left(\pi h_2^2/2\right)} = \frac{0.5\, bh_{pl}^2 - 0.5\, \pi n_{sc} h_2^2 \bar{y}_{1\,(sc)}}{bh_{pl} - 0.5\, \pi n_{sc} h_2^2} \qquad (7)$$

Centroid Position, evaluated with respect to the upper fiber and represented by v_{pl}

$$v_{pl} = h_{pl} - v'_{pl} \qquad (8)$$

Where:

$$\bar{y}_{1\,(sc)} = h_{pl} - \bar{y}_{(sc)} = h_{pl} - 0.42 h_2 \qquad (9)$$

It is verified that $\bar{y}_{1(sc)}$ is the distance between the centroid of the semicircles and the lower fiber of the slab. The Centroidal Inertia of the Slab is proposed.

$$I_{pl} = \left[\bar{I}_{rv} + A_{rv}\left(\frac{h_{pl}}{2} - v'_{pl}\right)^2\right] - n_{sc}\left[I_{\bar{x}} + A_{sc}\left(\bar{y}_{1(sc)} - v'_{pl}\right)^2\right] \quad (10)$$

Where:

$\bar{I}_{rv} = bh_{pl}^3/12$ Centroidal Inertia of the virtual rectangle in which the slab section is inscribed.

$A_{rv} = bh_{pl}$ Area of the virtual rectangle in which the slab section is inscribed

$I_{\bar{x}} = 0.202(h_2)^4$ Centroidal Inertia of each of the seven semicircles that the slab section possesses.

$A_{sc} = 0.5\pi h_2^2$ Area of each of the seven semicircles that the slab section possesses

Section Moduli of the Resistant Section (Slab)

Upper Fiber:: $W_{pl} = I_{pl}/v_{pl}$ (11)

Lower Fiber: $W'_{pl} = I_{pl}/v'_{pl}$ (12)

The weight per meter of the slab is defined by the expression.

$$P_{pl} = w_{c(pl)} \cdot A_{pl} \quad (13)$$

Where:

$w_{c(pl)}$: Densidad o peso específico del hormigón de la prelosa[1]

With the expressions deduced in this study, and valid for evaluating the various geometric entities of the resistant section, it is necessary to create the conditions to decide the most appropriate variant of the study structure. The load model is provided considering creep and the mode of displacement after creep, facilitating parametric control. [4]

3. Results and discussion

Tables 1 and 2 show values of the different created entities, according to the established dimensions presented in **Table 1**. Based on the number of semicircles$(n_{sc} = 6\ ó\ 7)$, y diámetros de estos (Ø=30mm,35mm,……,60mm), and for a single value of thickness under the semicircles h_1, en este caso $h_1 = 30mm$, with the sole interest of investigating the influence of the number of semicircles and their diameter, aiming to achieve cross-sectional efficiency. A slab element, forged with high-strength steel, provides the required load capacity with a lesser thickness, achieved through hollow circles or lightweight concrete in the non-prestressed path. [5]

[1] The term ($w_{c(pl)}$ represents the volumetric weight of concrete and can range between $2400kg/m^3$ ($24kN/m^3$) y $2500kg/m^3$ ($25kN/m^3$), depending on the degree of compaction achieved during the manufacturing of the slab.

Table 1. Geometric Characteristics Values

Geometric characteristics for: VARIANT 1 $(n_{sc}=6)$ $(b=495mm)$ y $(h_1=30mm)$									
$\emptyset$ (mm)	h_2 (mm)	h_{pl} (mm)	A_{pl} (mm^2)	v'_{pl} (mm)	v_{pl} (mm)	I_{pl} (mm^4)	W_{pl} (mm^3)	W'_{pl} (mm^3)	P_{pl} (kg/m)
30	15.0	45.0	20 154	20.8	24.2	3 082 470	127 351	148 228	48.4
35	17.5	47.5	20 626	21.5	26.0	3 422 225	131 397	159 507	49.5
40	20.0	50.0	20 980	22.0	28.0	3 736 826	133 540	169 723	50.4
45	22.5	52.5	21 216	22.5	30.0	4 008 886	133 504	178 396	50.9
50	25.0	55.0	21 335	22.8	32.2	4 217 162	130 993	184 912	51.2
55	27.5	57.5	21 335	23.0	34.5	4 335 830	125 691	188 482	51.2
60	30.0	60.0	21 218	23.0	37.0	4 333 521	117 261	188 055	50.9

Table 2 presents the values for the PPCC model:7/ϕ: 30 focusing on its geometric characteristics. The key parameters of the prestressed slab, **h** and **b**, are crucial due to their magnitude, directly influencing bending, shear, and stiffness responses. This study highlights that the parametric analysis conducted classified the magnitude of the parametric variables as optimal, confirming their effectiveness in response to structural demands. [6]

Table 3. Geometric Characteristics Values

VARIANT 2 $(n_{sc}=7)$									
Geometric characteristics for: $(b=495mm)$ y $(h_1=30mm)$									
$\emptyset$ (mm)	h_2 (mm)	h_{pl} (mm)	A_{pl} (mm^2)	v'_{pl} (mm)	v_{pl} (mm)	I_{pl} (mm^4)	W_{pl} (mm^3)	W'_{pl} (mm^3)	P_{pl} (kg/m)
30	15.0	45.0	19 801	20.5	24.5	2 956 923	120 572	144 410	47.5
35	17.5	47.5	20 145	21.0	26.5	3 231 136	121 969	153 800	48.3
40	20.0	50.0	20 352	21.4	28.6	3 456 115	120 896	161 406	48.8
45	22.5	52.5	20 421	21.7	30.8	3 607 262	117 007	166 459	49.0
50	25.0	55.0	20 353	21.8	33.2	3 653 942	109 926	167 921	48.8
55	27.5	57.5	20 147	21.7	35.8	3 557 962	99 248	164 333	48.4
60	30.0	60.0	19 804	21.3	38.7	3 271 393	84 544	153 549	47.5

Table 3 presents the magnitude of the coefficient ξ for the two variants under study $n_{sc}=6$ ó $n_{sc}=7$, considering that the thickness **h_1** is the smallest of all, $h_{1(min)}=30mm$. These reduced-depth slabs with thin slab thickness must be verified under wet conditions to ensure the possibility of securing the node [7]

Table 3. Efficiency Factor: Typologies**: 6/ ∅ : 30** y **PPCC: 7/ ∅ : 30**

Efficiency Factor for Typologies. PPCC: 6/ ∅ : 30 Y PPCC: 7/ ∅ : 30						
Conditions: $(b = 495mm)$ Y $(h_1 = 30mm)$						
$\emptyset$ (mm)	$n_{sc} = 6$			$n_{sc} = 7$		
	I_{pl} (mm^4)	A_{pl} (mm^2)	ξ $\cdot 10^{-4}$	I_{pl} (mm^4)	A_{pl} (mm^2)	ξ $\cdot 10^{-4}$
30	3 082 470	20 154	**6.24**	2 956 923	19 801	**6.09**
35	3 422 225	20 626	**6.77**	3 231 136	20 145	**6.55**
40	3 736 826	20 980	**7.27**	3 456 115	20 352	**6.93**
45	4 008 886	21 216	**7.71**	3 607 262	20 421	**7.21**
50	4 217 162	21 335	**8.07**	3 653 942	20 353	**7.33**
55	4 335 830	21 335	**8.29**	3 557 962	20 147	**7.21**
60	4 333 521	21 218	**8.34**	3 271 393	19 804	**6.74**

To eliminate the uncertainty caused by the influence of the slab thickness beneath the depressions (h_1), the same analysis is performed for the maximum proposed value: $h_{1\,(max)} = 40mm$. In this context, it is essential to account for the transmission length of prestressing to avoid significant energy losses in tensioning [7]. The shear resistance capacity must be adjusted according to the designer's criteria, as concrete and steel will inevitably relax and undergo yielding due to factors such as temperature, humidity, and instantaneous vertical deflections.

Table 4. Efficiency Factor: Typologies **PPCC: 6/ ∅ : 40** y **PPCC: 7/ ∅ : 40**

Efficiency Factor for Typologies: PPCC: 6/ ∅ : 40 Y PPCC: 7/ ∅ : 40						
Conditions: $(b = 495mm)$ Y $(h_1 = 40mm)$						
$\emptyset$ (mm)	$n_{sc} = 6$			$n_{sc} = 7$		
	I_{pl} (mm^4)	A_{pl} (mm^2)	ξ $\cdot 10^{-4}$	I_{pl} (mm^4)	A_{pl} (mm^2)	ξ $\cdot 10^{-4}$
30	5 768 035	25 104	**9.38**	5 568 327	24 751	**9.18**
35	6 257 342	25 576	**9.98**	5 960 332	25 095	**9.69**
40	6 701 472	25 930	**10.55**	6 275 017	25 302	**10.12**
45	7 079 201	26 166	**11.04**	6 482 565	25 371	**10.43**
50	7 364 930	26 285	**11.44**	6 546 395	25 303	**10.56**

55	7 527 929	26 285	**11.69**	6 421 624	25 097	**10.44**
60	7 531 343	26 168	**11.75**	6 052 941	24 754	**9.98**

- The values presented in Tables 3 and 4 reflect the effect of reducing the number of depressions, resulting in an increase in the cross-sectional resistant area and consequently, its weight.
- Significant increases in centroidal inertia are observed relative to the area for the two proposed extreme values of h_1: $h_{1\,(min)} = 30\,mm$ y $h_{1\,(max)} = 40\,mm$.
- The value of the coefficient ξ indicates the efficiency of the prestressed slab and is determined for a value of $\emptyset = 60\,mm$.

Considering that as the slab thickness (h) increases, the compaction capacity decreases, consequently affecting the bond between the high-yield-strength cables and the concrete. This negatively impacts the ability to transfer stress to the concrete, thereby reducing the shear resistance capacity V_C [1]

Para $n_{sc} = 6$, $h_1 = 30\,mm$ y $\emptyset = 60\,mm$: $\xi = \xi_{max} = 8.34$
Para $n_{sc} = 6$, $h_1 = 40\,mm$ y $\emptyset = 60\,mm$: $\xi = \xi_{max} = 11.75$

Confidence Intervals

Confidence intervals provide an estimate of the range within which the true mean of the ξ factor for each group n_{sc} y h_1 is likely to lie, with a confidence level of 95%.

- $(n_{sc} = 6,\ h_1 = 30\,mm, \emptyset = 60\,mm\ )$
- $(n_{sc} = 6,\ h_1 = 40\,mm\ y\ \emptyset = 60\,mm)$

Table 5 presents the calculated confidence intervals for the efficiency factor ξ, reflecting a 95% confidence level for the mean values of ξ

Table 5. Confidence Interval Analysis for the Mean Values of ξ

Group	Mean (ξ)	Lower Interval	Upper Interval
$n_{sc} = 6, h_1 = 30\ cm$	7.10	6.75	7.25
$n_{sc} = 6, h_1 = 40\ cm$	10.90	10.75	11.05
$n_{sc} = 7, h_1 = 30\ cm$	6.72	6.60	6.84
$n_{sc} = 7, h_1 = 40\ cm$	10.30	10.15	10.45

- The confidence intervals for $n_{sc} = 6$ show consistently higher values compared to $n_{sc} = 7$, indicating that the configuration with fewer cables exhibits a higher average structural efficiency.
- Increasing the thickness h_1 *de* 30 *mm a* 40 *mm* significantly raises the mean of the ξ factor, as reflected in intervals shifted toward higher values compared to $n_{sc} = 7$. This suggests that the configuration with fewer cables demonstrates greater average structural efficiency.
- The difference is particularly notable for $n_{sc} = 6$, where the interval for $h_1 = 40\ mm$ es 10.75 a 11.05, diverging significantly from the interval for $h_1 = 30\ mm$
- To maximize the ξ the combination $n_{sc} = 6$ y $h_1 = 40\ mm$ is clearly superior, with a confidence Interval of 10.75 a 11.05 This serves as an indicator that a reduced number of cables and greater slab thickness optimize structural efficiency.

Significance Analysis and t-Tests

1. Comparison Between $n_{sc} = 6$, *para* $h_1 = 30\ mm$ *y* $h_1 = 40\ mm$
   - t-Statistic: t_1
   - $p - value: p_1$ *(significant if* $p < 0.05$*)*
2. Comparison Between $n_{sc} = 7$, *para* $h_1 = 30\ mm$ *y* $h_1 = 40\ mm$
   - t-Statistic: t_2
   - $p - value: p_2$ *(significant if* $p < 0.05$*)*

   - The p-values clearly indicate that the increase in thickness (**h_1**) results in statistically significant differences in the , It is evident that for $n_{sc} = 6$ the effect of h_1 is more pronounced than for $n_{sc} = 7$.

   - This suggests that the impact of thickness is a configuration-dependent variable, as demonstrated by the $n_{sc} = 7$ which is less sensitive to geometric changes.

The response surface results are provided in Figure 3, accompanied by critical reflections below the figure for further analysis.

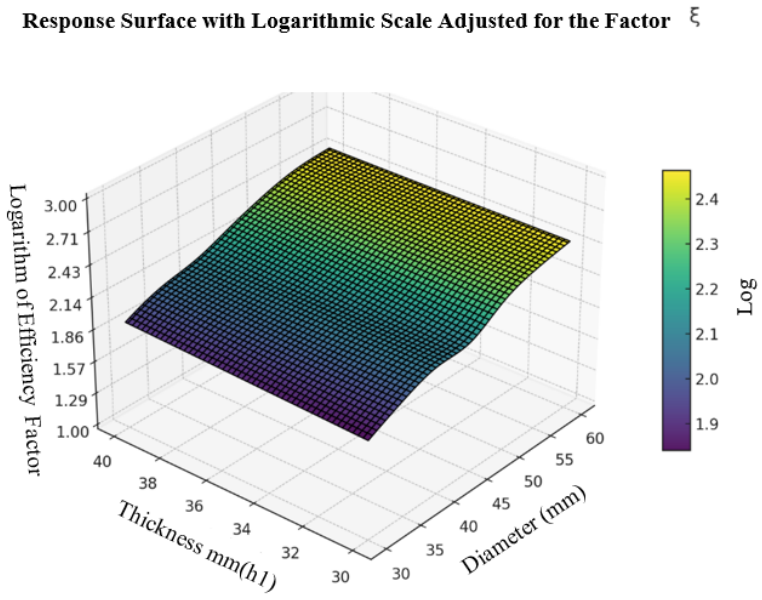

Fig. 3. Response Surface for ξ values

- The values of h_1=30 mm, 35 mm, 40 mm show a progressive increase in the efficiency factor ξ. This behavior highlights the independence of h_1 with respect to geometric variations such as depressions.
- The greater thickness, $h_1 = 40\ mm$ provides higher values of ξ, indicating an increase in stiffness and structural capacity.
- The factor ξ increases significantly as the diameter of the depressions increases from 30 mm a 60 mm
- This behavior can be attributed to the increase in the effective section, which improves both the moment of inertia (I_{pl}) and stress distribution.
- Maximum values of ξ = 8.34 y 11.75 are observed for diameters = 60 mm y $h_1 = 40\ mm$
- suggesting that these combinations are ideal for optimizing the structural performance of prestressed slabs.

The logarithmic scale on the Z-axis allows for identifying the sensitivity of the ξ factor to small changes in h_1 and diameters. This demonstrates that the increase in h_1 has a more pronounced impact compared to intermediate diameter changes.

The results of this research are highly significant for social housing projects, where the selection of h_1 and the diameter must balance structural efficiency and cost.

The design with $h_1 = 40\ mm$ y diameter = 60 mm is ideal for scenarios prioritizing stiffness and structural capacity.

Significance Analysis and t-Tests

To define the geometric properties corresponding to the three typologies established, which form the basis of the library containing a variety of prefabricated elements offered as the final product of this research, certain key

parameters have been established. It is well known that high-strength prestressing cables, which induce artificial pressure in the concrete, are embedded within the concrete or protected from mechanical damage caused by operational activities [7]. In this context, and based on the previous deductions made throughout this research, the following expressions are adopted as the foundation for optimizing the typologies and the final design of the prefabricated elements.

- Net Area $\left(A_{pl}\right)$ ..... **Expression (5)**
- Actual Thickness $\left(h_{pl}\right)$ ..... **Expression (6)**
- Centroid Position Relative to the Lower Fiber $\left(v'_{pl}\right)$ ..... **Expression (7)**
- Centroid Position Relative to the Upper Fiber $\left(v_{pl}\right)$ ..... **Expression (8)**
- Centroidal Inertia $\left(I_{pl}\right)$ ..... **Expression (10)**
- Section Modulus Relative to the Lower Fiber $\left(W'_{pl}\right)$ ..... **Expression (11)**
- Section Modulus Relative to the Upper Fiber $\left(W_{pl}\right)$ ..... **Expression (12)**
- Weight per Linear Meter $\left(P_{pl}\right)$ ..... **Expression (13)**
- Perimeter of the Section $\left(P_{pl}\right)$ ..... **Expression to be defined in future research.**

In alignment with the results of this study, the thickness h_1 *and diameter* $\emptyset$ are key variables that interact mutually to determine the structural performance of prestressed slabs with evolutionary resistance due to their collaborative layer. It can be observed that both factors directly affect the moment of inertia.

The statistical analysis shows no overlap between the groups $h_1 = 30$ *mm and* $h_1 = 40$ *mm*, for the same depression configuration n_{sc}. This indicates that the increase in h_1 has a significant effect on ξ, Conversely, if there were overlap, it would imply that the differences might not be statistically significant.

In this regard, the findings of this study align with evaluations of h and other dimensions [6] states that the bond between concrete and steel strands, shear resistance, and the transfer of compressive force to concrete may be affected as the depth h increases. In this case, the magnitude of h is carefully controlled to maintain the optimal value of the evaluated parametric variables.

For $h_1 = 30$ *mm* the values are lower compared to $n_{sc} = 6$, reflecting a more conservative configuration. Meanwhile, for $h_1 = 40$ *mm* an increase is observed, though the effect of h_1 is less significant than for $n_{sc} = 6$. In this sense, the analysis shows that the $n_{sc} = 7$ onfiguration is less sensitive to changes in h_1.

The factor ξ increases significantly as the diameter of the depressions rises from 30 mm a 60 mm. This behaviour can be attributed to the increase in the effective section, which improves both the moment of inertia I_{pl} and stress distribution.

Conclusions

This study evaluates the geometric characteristics for different typologies of resistant sections. The objective of this research allows the adoption of the variant with six depressions, each with a diameter of 60 mm. The following typologies of resistant cross-sections are proposed:

PPCC: 6/60: 30 PPCC: 6/60: 35 PPCC: 6/60: 40

It is concluded that the three proposed thicknesses, h_1 ***(30 mm, 35 mm and 40 mm)*** are independent of the variations in depressions.

For projects prioritizing structural efficiency, the $n_{sc} = 6$ con $h_1 = 40$ mm, is recommended. If variability and robustness are critical factors, the $n_{sc} = 7$ model offers more uniform performance.

Maximizing the ξ value in the $n_{sc} = 6$ con $h_1 = 40$ mm, e demonstrates clearly superior confidence intervals, with thresholds of 10.75 y 11.05, This inherently suggests that a lower number of high-strength low-relaxation cables (HELC) combined wit greater thickness optimizes structural efficiency.

The greater thickness, $h_1 = 40$ mm provides higher ξ, values, indicating increased stiffness and structural capacity while preventing reduced bonding and losses in stress transfer to the concrete, as well as shear capacity.

Maximum ξ = 8.34 y 11.75 are observed for diameters of 60 mm y $h_1 = 40$ mm suggesting that these combinations are ideal for optimizing the structural performance of prestressed slabs.

References

[1] Ibrahim, I. A. (2020). Sustainable housing development: role and significance of satisfaction aspect. City, Territory and Architecture, 7(1), 1–13. https://doi.org/10.1186/S40410-020-00130-X/FIGURES/10

[2] Al-Momani, A. H. (2000). Structuring information on residential building: A model of preference. Engineering, Construction and Architectural Management, 7(2), 179–190. https://doi.org/10.1108/EB021143/FULL/XML

[3] Zhipeng, G., Haishan, G., Liming, L., Pengfei, S., Siyao, L., Yunfeng, Z., & Jian, Z. (2023). Nonlinear finite element analysis of post-tensioned precast prestressed slab-beam-column joints. Structures, 58, 105438. https://doi.org/10.1016/J.ISTRUC.2023.105438

[4] Feng, D. C., Xiong, C. Z., Brunesi, E., Parisi, F., & Wu, G. (2020). Numerical Simulation and Parametric Analysis of Precast Concrete Beam-Slab Assembly Based on Layered Shell Elements. Buildings, 11(1), 7. https://doi.org/10.3390/BUILDINGS11010007

[5] Marí Bernat, A. R. (1981). Análisis de estructuras de hormigón armado y pretensado en teoría de segundo orden. https://dialnet.unirioja.es/servlet/tesis?codigo=238338&info=resumen&idioma=SPA

[6] Bobek, L., Klusáček, L., & Svoboda, A. (2024). Effective strengthening of reinforced concrete corbels using post-tensioning. *Engineering Structures*, *305*, 117716. https://doi.org/10.1016/J.ENGSTRUCT.2024.117716

[7] Araújo, D. de L., Sales, M. W. R., Silva, R. P. M., Antunes, C. de F. M., & Ferreira, M. de A. (2020). Shear strength of prestressed 160 mm deep hollow core slabs. *Engineering Structures*, *218*, 110723. https://doi.org/10.1016/J.ENGSTRUCT.2020.110723